

Articles

Highly Efficient Blue-Light-Emitting Diodes from Polyfluorene Containing Bipolar Pendant Groups

Ching-Fong Shu,^{*,†} Rajasekhar Dodda, and Fang-Iy Wu

Department of Applied Chemistry, National Chiao Tung University, Hsin-Chu, Taiwan 30035, R. O. C.

Michelle S. Liu and Alex K.-Y. Jen*

Department of Materials Science and Engineering, Box 352120, University of Washington, Seattle, Washington 98195-2120

Received February 19, 2003; Revised Manuscript Received May 26, 2003

ABSTRACT: A highly efficient blue-light-emitting copolymer with bulky hole-transporting triphenylamine (TPA) and electron-transporting oxadiazole (OXD) pendant groups at the C-9 position of fluorene was synthesized. The results from photoluminescence and electrochemical measurements reveal that both the side chains and the polyfluorene main chain retain their own electronic characteristics in the copolymer. It shows a pure blue emission with no aggregates or excimers formed even after being annealed at 150 °C under nitrogen for 20 h. In addition, it also demonstrates improved charge injection and balanced charge transport in electroluminescence. The maximum external quantum efficiency of a single-layer device using this copolymer as the emitting layer is 1.21% (at a brightness of 354 cd/m² with driving voltage of 7.6 V). The maximum luminance of the device reaches 4080 cd/m² at a bias of 12.0 V and a current density of 640 mA/cm².

Introduction

The development of blue-light-emitting polymers has been the subject of intense academic and industrial research due to their potential for full-color flat panel displays. They can be used either as the active layer in polymer light-emitting diodes (PLEDs) or as the host material for generating other colors through energy transfer to lower energy fluorophores.^{1–4} Polyfluorenes (PF), with their high thermal stability and exceptionally high solution and solid-state fluorescence quantum yields, are very promising candidates for blue LEDs.^{4–8} Recently, a fluorene homopolymer, poly(9,9-di-*n*-octylfluorene) (POF), has been demonstrated as an effective blue emitter.⁹ However, this type of polyfluorene tends to form aggregates and/or excimers during device fabrication and operation, leading to both a red-shifted emission and lower efficiency.¹⁰ This can be overcome by introducing bulky substituents at the C-9 position of the fluorene.^{11–15} Such structural features could minimize the close chain packing of molecules in solid state. In addition, the saturated sp³ carbon (C-9) on the fluorene ring can also effectively block the conjugation between the side chains and the polymer backbone. As a result, the pure blue emission from the PF main chain can be preserved.

More recently, we reported the synthesis of a fluorene-based alternating copolymer, PF-OXD, which contains

oxadiazole (OXD) moieties with their phenyl end group directly attached to the C-9 carbon in every alternating fluorene unit.¹⁵ The electron-deficient OXD derivatives were introduced to improve both electron injection and transport. The results from the photoluminescence (PL) measurements of the isothermally heated PF-OXD thin film (150 °C for 20 h) show that the commonly observed aggregate/excimer formation in polyfluorene was effectively suppressed in this polymer due to its 3-D structure. The LED device using this polymer also shows a low turn-on voltage, high brightness, and efficiency due to a more balanced charge recombination in the polymer emissive layer. However, the ionization potential for PF-OXD is 5.76 eV, which is very similar to that of POF (5.8 eV). This means that there is a significant energy barrier for hole injection from the conducting polymer, poly(ethylenedioxythiophene):poly(styrenesulfonate) (PEDOT:PSS)-modified ITO (~5.2 eV), to PF-OXD, and it needs to be improved in order to further enhance the device performance.

Here we report the synthesis, characterization, and device performance of a new statistical copolymer PF-TPA-OXD containing both electron-transporting OXD moieties and hole-transporting triphenylamine (TPA) units that are functionalized at the C-9 position of fluorene. These bipolar substituents provide both functions of suppressing aggregation and improving charge injection simultaneously.

Experimental Section

Materials. 2,7-Dibromofluorenone (**1**),¹⁶ 4,4'-dibutyltriphenylamine (**2**),¹⁷ oxadiazole monomer (**4**),¹⁵ and 2,7-bis-

[†] Dedicated to Professor Kwang-Ting Liu on the occasion of his 65th birthday.

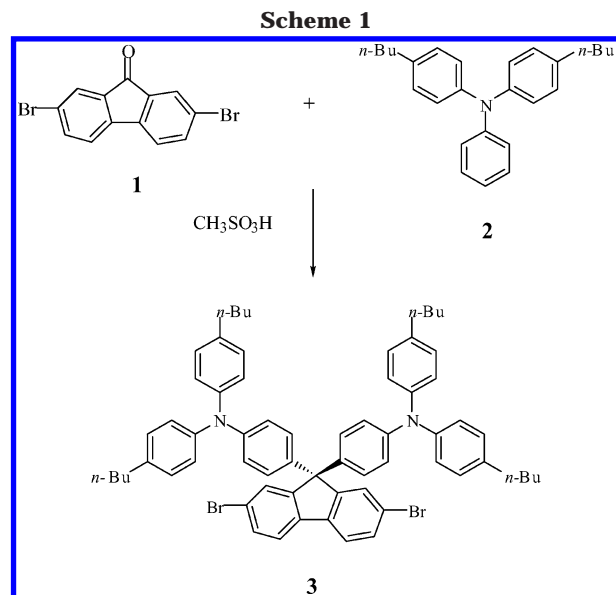
* To whom correspondence should be addressed.

(4,4,5,5-tetramethyl-1,3,2-dioxaborolan-2-yl)-9,9-dioctylfluorene (**5**)¹⁸ were synthesized according to literature procedures.

9,9-Bis(4-di(4-butylphenyl)aminophenyl)-2,7-dibromofluorene (3). To a mixture of 2,7-dibromofluorenone (315 mg, 930 μ mol) and 4,4'-dibutyltriphenylamine (1.0 g, 2.8 mmol) was added methanesulfonic acid (60 μ L, 0.93 mmol). The reaction mixture was then heated at 140 °C under nitrogen for 12 h. The cooled mixture was diluted with dichloromethane and washed with aqueous sodium carbonate. The organic phase was dried over MgSO₄, and the solvent was evaporated. The crude product was purified by column chromatography, eluting with hexane/ethyl acetate (8:2), followed by recrystallization from acetone to afford **3** (0.50 g, 52%) as white crystals. ¹H NMR (300 MHz, CDCl₃): δ 0.91 (12 H, t, J = 7.4 Hz), 1.34 (8 H, m), 1.56 (8 H, m), 2.54 (8 H, t, J = 7.7 Hz), 6.84 (4 H, d, J = 8.7 Hz), 6.94 (4 H, d, J = 8.7 Hz), 6.97 (8 H, d, J = 8.4 Hz), 7.03 (8 H, d, J = 8.4 Hz), 7.44 (2 H, dd, J = 8.1, 1.5 Hz), 7.50 (2 H, d, J = 1.5 Hz), 7.54 (2 H, d, J = 8.1 Hz). ¹³C NMR (75 MHz, CDCl₃): δ 153.7, 147.1, 145.2, 137.9, 137.7, 136.6, 130.7, 129.4, 129.1, 128.5, 124.8, 121.7, 121.6, 121.4, 64.6, 35.0, 33.6, 22.4, 14.0. Anal. Calcd for C₆₅H₆₆Br₂N₂: C, 75.43; H, 6.43; N, 2.71. Found: C, 75.41; H, 6.56; N, 2.25.

PF-TPA-OXD. To a solution of **3** (161 mg, 156 μ mol), **4** (137 mg, 156 μ mol), and **5** (200.0 mg, 312 μ mol) in toluene (4.0 mL) were added aqueous potassium carbonate (2.0 M, 4.0 mL) and aliquate (20 mg). The above solution was degassed, and tetrakis(triphenylphosphine)palladium (10 mg, 5.5 mol %) was added in one portion under a nitrogen atmosphere. The solution was refluxed under nitrogen for 3 days. The end groups were capped by refluxing for 12 h each with phenylboronic acid (40 mg, 0.33 mmol) and bromobenzene (52 mg, 0.33 mmol). After this period, the mixture was cooled and poured into a mixture of methanol and water (150 mL, 7:3 v/v). The crude polymer was filtered, washed with excess methanol, and dried. The polymer was dissolved in CHCl₃ (2.0 mL), filtered, and precipitated into methanol (150 mL). The precipitate was collected, washed with acetone for 24 h using a Soxhlet apparatus, and dried under vacuum to give PF-TPA-OXD (270 mg, 73%). ¹H NMR (300 MHz, CDCl₃): δ 0.69–0.75 (20 H, m), 0.89 (12 H, t, J = 7.5 Hz), 1.02–1.19 (40 H, m), 1.24–1.40 (26 H, m), 1.57 (8 H, m), 2.04 (8 H, m), 2.54 (8 H, m), 6.89–7.16 (24 H, m), 7.51–7.84 (30 H, m), 7.93–8.11 (10 H, m). ¹³C NMR (75 MHz, CDCl₃): δ 164.8, 164.1, 155.4, 152.9, 151.9, 151.8, 150.9, 149.3, 146.8, 145.4, 141.9, 141.1, 140.4, 140.3, 139.8, 139.1, 138.9, 138.6, 137.6, 129.1, 129.0, 128.9, 127.7, 127.4, 127.3, 126.8, 126.3, 126.1, 124.7, 123.0, 121.9, 121.4, 121.1, 120.9, 120.4, 120.1, 65.9, 64.8, 55.4, 40.4, 35.2, 35.1, 33.7, 31.8, 31.2, 30.0, 29.2, 23.9, 22.6, 22.4, 14.1, 14.0. Anal. Calcd for C₁₇₂H₁₈₆N₆O₂: C, 87.19; H, 7.91; N, 3.55. Found: C, 86.27; H, 7.73; N, 3.11.

Characterization. ¹H and ¹³C NMR spectra were recorded on a Varian Unity 300 MHz or a Bruker-DRX 300 MHz spectrometer. Mass spectra were obtained on a JEOL JMS-SX/SX 102A mass spectrometer. Size exclusion chromatography (SEC) was carried out on a Waters chromatography unit interfaced to a Waters 410 differential refractometer. Three 5 μ m Waters styragel columns (300 \times 7.8 mm) connected in series in the decreasing order of pore size (10⁴, 10³, and 10² Å) were used with THF as eluent, and standard polystyrene samples were used for calibration. Differential scanning calorimetry (DSC) was performed on a SEIKO EXSTAR 6000 DSC unit using a heating rate of 10 °C min⁻¹ and a cooling rate of 30 °C min⁻¹. Samples were scanned from 30 to 350 °C and then cooled to 30 °C and scanned for second time from 30 to 350 °C. Glass transition temperatures (T_g) were determined from the second heating scan. Thermogravimetric analysis (TGA) was made on a Du Pont TGA 2950 instrument. The thermal stability of the samples was determined under nitrogen by measuring weight loss while heating at a rate of 20 °C min⁻¹. UV-vis spectra were measured with a HP 8453 diode array spectrophotometer. Photoluminescence spectra were obtained on a Hitachi F-4500 luminescence spectrometer. The PL quantum yield (Φ_f) in toluene solution was measured by excitation of the respective polymer solutions at 365 nm and compared with the solution emission of the 9,10-diphen-

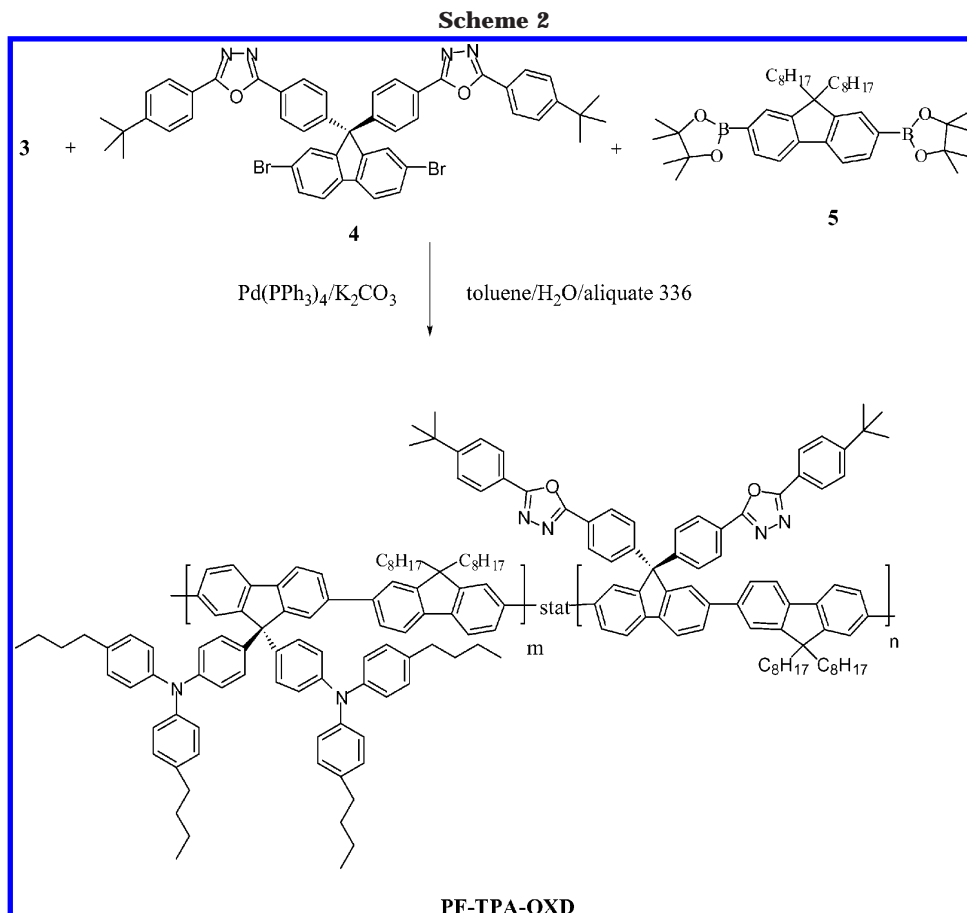


ylanthracene (ca. 5 \times 10⁻⁶ M solution in cyclohexane, Φ_f = 0.9).¹⁹ The solid-state fluorescence yields were determined by comparing the fluorescence of the respective polymer films (λ_{exc} = 375 nm) with the film of 9,10-diphenylanthracene in poly(methyl methacrylate) (10⁻³ M) on quartz substrates. Cyclic voltammetry measurements of the polymer films were performed on a BAS 100 B/W electrochemical analyzer in acetonitrile with 0.1 M tetrabutylammonium hexafluorophosphate (TBAPF₆) as the supporting electrolyte at a scan rate of 50 mV/s. The potentials were measured against an Ag/Ag⁺ (0.01 M AgNO₃) reference electrode with ferrocene as the internal standard. The onset potentials were determined from the intersection of two tangents drawn at the rising current and background current of the cyclic voltammogram.

Device Fabrication and Testing. The devices were fabricated on ITO substrates that had been ultrasonicated sequentially in detergent, methanol, 2-propanol, and acetone and had been treated with O₂ plasma for 10 min before use. All the evaporation of the metal electrodes was carried out in a vacuum evaporator inside an argon atmosphere drybox. A hole-injecting layer, PEDOT (Bayer Corp.), was spin-coated at a spin rate of 4000 rpm from its water solution (1.3 wt %) onto the ITO substrates and cured at 160 °C for 10 min under nitrogen. Then a layer of copolymer was spin-coated from its toluene solution (2 wt %) at 1600 rpm. The thickness of the films was measured on a Sloan Dektak 3030 surface profilometer. The thickness of PEDOT was about 30 nm, and the thickness of the polymer layer was around 60 nm. A layer of 30 nm thick calcium (Ca) cathode was then vacuum-deposited at below 1 \times 10⁻⁶ Torr through a mask, and another protecting layer of 120 nm thick silver (Ag) was vacuum-deposited. The device testing was carried out in air at room temperature. Current-voltage characteristics were measured on a Hewlett-Packard 4155B semiconductor parameter analyzer. The power of EL emission was measured using a Newport 2835-C multifunction optical meter. Photometric units (cd/m²) were calculated using the forward output power and the EL spectra of the devices, assuming Lambertian distribution of the EL emission.²⁰

Results and Discussion

Polymer Synthesis and Characterization. As shown in Scheme 1, the TPA monomer **3** was synthesized by an acid-catalyzed condensation reaction between 2,7-dibromofluorenone (**1**)¹⁶ and 4,4'-dibutyltriphenylamine (**2**).¹⁷ This method resembles the similar procedure that was used recently by Mullen et al. to introduce triphenylamine groups onto the C-9 position of fluorene.¹² The OXD monomer **4** was prepared as



reported previously.¹⁵ The statistical polyfluorene copolymer PF-TPA-OXD was synthesized from a Suzuki coupling reaction between the dibromides **3** and **4**, and the diboronate **5**,¹⁸ with a mole ratio of 1.0:1.0:2.0 (Scheme 2). The copolymerization was carried out using Pd(PPh₃)₄ as the catalyst in a mixture of toluene and aqueous K₂CO₃ (2.0 M) in the presence of Aliquat 336 as a phase transfer reagent. The structure of the obtained polymer was confirmed by ¹H and ¹³C NMR spectroscopy. On the basis of the integrations of the aliphatic protons, the composition of monomers **3**, **4**, and **5** present in this copolymer was estimated as 1.00:1.04:1.98, which matched very well with the feed ratio. In the ¹³C NMR spectrum, there are three signals at δ 64.8, 65.9, and 55.4, which correspond to the C-9 carbons of the three different fluorene units in PF-TPA-OXD. These signals are superimposed with the C-9 carbon signals of monomers **3**, **4**, and **5**.

The polyfluorene copolymer, PF-TPA-OXD, is readily soluble in common organic solvents, such as toluene, chloroform, THF, etc. The molecular weights of the polymer were determined by size exclusion chromatography (SEC) analysis, using THF as the eluent, and calibrated against polystyrene standards. It possesses a number-average molecular weight (M_n) of approximately 1.1×10^4 , with a polydispersity index of 2.2. The thermal properties of PF-TPA-OXD were investigated by differential scanning calorimetry (DSC) and thermogravimetric analysis (TGA). A distinct glass transition temperature (T_g) was observed at 166 °C in Figure 1. This relatively high T_g is essential for polymers used as emissive materials for light-emitting applications.²¹ As revealed by TGA, the polymer also exhibits good thermal stability with 5% weight loss occurring at 440 °C.

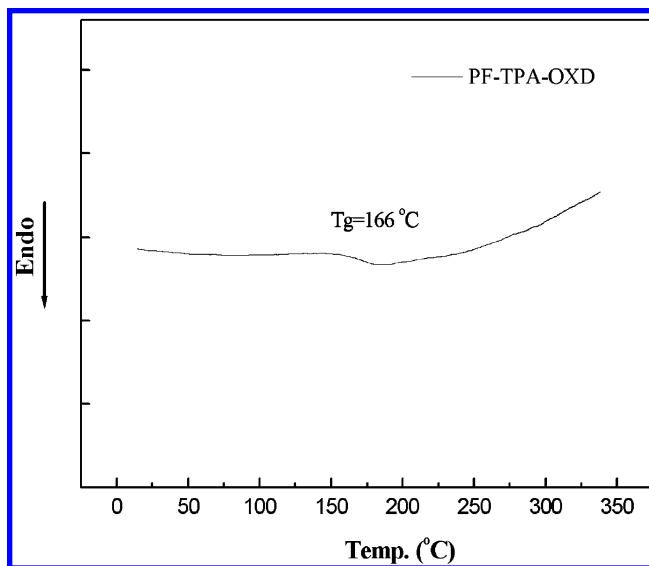


Figure 1. Differential scanning calorimetry (DSC) data of PF-TPA-OXD (heating rate, 10 °C/min) under nitrogen.

Optical Properties. The absorption and PL spectra of PF-TPA-OXD in diluted solution and in solid state are shown in Figure 2. PF-TPA-OXD in THF solution exhibits an absorption with a λ_{max} at 389 nm due to a $\pi-\pi^*$ transition derived from the conjugated polyfluorene backbone. An additional absorption band around 300 nm is originated from the combined absorption from the TPA and OXD pendant groups since the triarylamine **2** and 2,5-di(4-*tert*-butylphenyl)-1,3,4-oxadiazole (OXD), in THF, have an absorption with λ_{max} at 302 and 298 nm, respectively. It is worth noting that no absorption bands are observed in the longer wavelength region

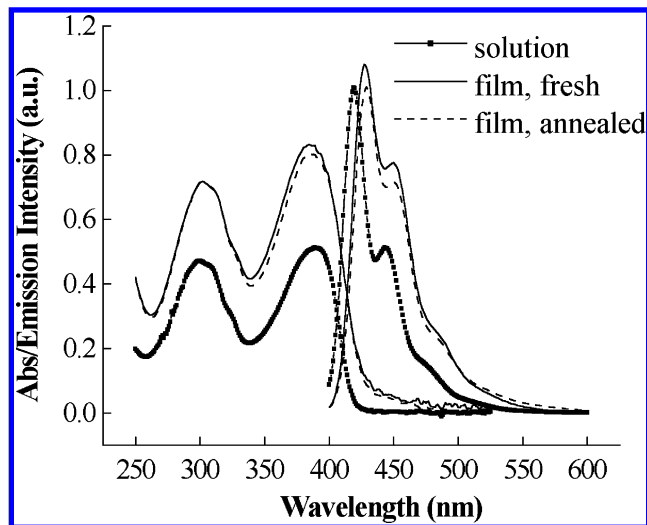


Figure 2. UV-vis absorption and PL (excited at 390 nm) spectra of PF-TPA-OXD in THF solution and in solid state; also included are the absorption and PL spectra of the PF-TPA-OXD film after annealing at 150 °C for 20 h under nitrogen (the intensities are relative to those of a fresh film).

(400–600 nm), which would correspond to the charge-transfer transition from the electron-rich TPA to the electron-deficient OXD moieties. Upon excitation of the polyfluorene main chain at 390 nm, the emission spectrum displays a vibronic fine structure with two sharp bands at 420 and 444 nm. The PL spectrum is nearly identical to that obtained from POF in THF ($\lambda_{\text{max}} = 418, 442$ nm). This result suggests that the incorporation of TPA and OXD groups onto fluorene units via the C-9 carbon does not perturb the main chain conjugation. The fluorescence quantum yield (Φ_{FL}) of PF-TPA-OXD in toluene solution ($\lambda_{\text{exc}} = 365$ nm) was estimated to be 0.95, using 9,10-diphenylanthracene ($\Phi_{\text{f}} = 0.9$) as the standard.¹⁹ In comparison to dilute solutions, the emission spectrum of a film spin-coated on a quartz substrate shows a slightly bathochromic shift, with maxima at 426 and 450 nm. The PL quantum yield of the film was measured to be 0.42 using the same standard in poly(methyl methacrylate).

Figure 2 also shows the absorption and PL spectra of a PF-TPA-OXD film thermally annealed at 150 °C under a nitrogen atmosphere for 20 h. Both spectra remain almost unchanged after the thermal treatment. In contrast, previous reports showed that the annealing of a POF film, in which each repeating fluorene unit contains two flexible *n*-octyl chains at C-9, results in not only a bathochromical shift in PL wavelength and a significant reduction in emission intensity but also the appearance of an additional emission band between 500 and 600 nm.^{22,23} The absence of any low-energy emission band after thermal annealing in PF-TPA-OXD could be attributed to the attachment of bulky TPA and OXD moieties onto the C-9 position of the fluorene units. The resulting 3-D rigid structure may prevent π -stacking between polymer chains and suppress the formation of aggregates/excimers in the solid state. The higher T_g of the PF-TPA-OXD also accounts for the better thermal stability of the polymer film.

As shown in Figure 3, there are reasonable spectral overlaps between the emission bands of compounds **2** ($\lambda_{\text{max}} = 366$ nm), OXD ($\lambda_{\text{max}} = 347, 361$ nm), and the absorption band of the conjugated main chain of PF-TPA-OXD, indicating that there may be energy transfer from the excited TPA and OXD side chains to the

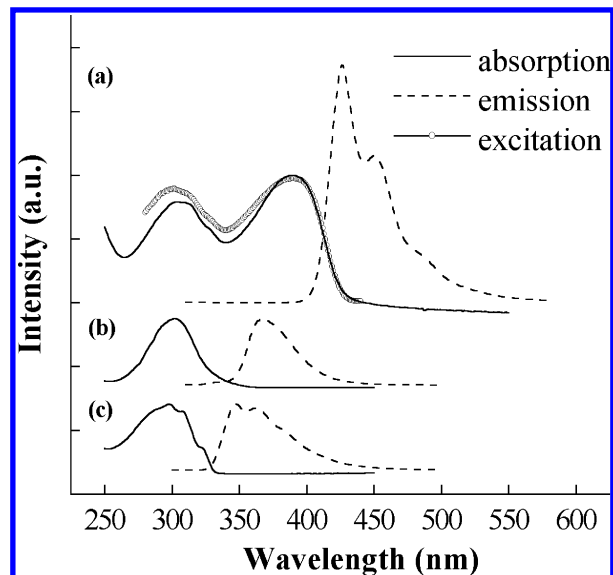


Figure 3. UV-vis absorption, PL (excited at 300 nm), and excitation (monitored emission at 450 nm) spectra of a PF-TPA-OXD film (a); UV-vis absorption and PL (excited at 300 nm) spectra of compounds **1** (b) and **6** (c) in THF solution.

polyfluorene backbone.²⁴ Upon irradiation at 300 nm, attributed to the TPA and OXD moieties, the PF-TPA-OXD film exhibits a blue fluorescence around 440 nm, which is the same as that under excitation of the PF backbone at 390 nm (Figure 2). There is no luminescence from the side chains can be detected at around 360 nm. In addition, the excitation spectrum of PF-TPA-OXD, monitored at 450 nm, is a perfectly superimposed image of the absorption spectrum. These results reveal that the energy transfer from the excited pendant groups to the PF backbone is very efficient and contributes significantly to the emission intensity of the main chain.

Redox Properties. Cyclic voltammetry (CV) of the polymer film coated on a glassy carbon electrode was performed in an electrolyte of 0.1 M tetrabutylammonium hexafluorophosphate (TBAPF₆) in acetonitrile using ferrocene as the internal standard. During the anodic scan, a reversible oxidation derived from the TPA moiety was observed at 0.61 V (E°) with the onset potential at 0.50 V followed by a quasi-reversible oxidation with a peak potential at 1.10 V, which can be assigned as the oxidation of the PF backbone. In the cathodic sweep, a quasi-reversible reduction derived from the OXD pendant group exhibited an onset potential at -2.26 V, while the reduction of the main chain is irreversible and the peak potential occurred at -2.92 V (Figure 4). On the basis of the onset potentials of the oxidation and reduction, the HOMO and LUMO energy levels of PF-TPA-OXD were estimated to be at -5.30 and -2.54 eV, respectively, with regard to the energy level of the ferrocene reference (4.8 eV below the vacuum level).²⁵ The high-lying HOMO and low-lying LUMO levels of PF-TPA-OXD may originate from the electron-rich and electron-deficient nature of the TPA and OXD moieties, respectively. The HOMO energy level of this polymer is similar to what has been reported for a TPA-substituted PF (-5.34 eV).¹² The LUMO level is close to those reported for a OXD-substituted PF (-2.47 eV)¹⁵ and for 2-(4-biphenyl)-5-(4-*tert*-butylphenyl)-1,3,4-oxadiazole (PDB) (-2.4 eV).²⁶ The electrochemical measurements reveal that both the side chains and the main chain do retain their own electronic characteristics in

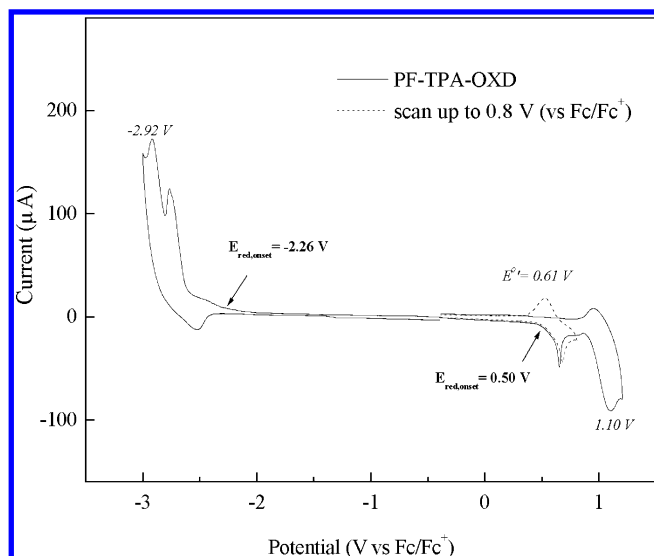


Figure 4. Cyclic voltammogram of PF-TPA-OXD film coated on a glassy carbon electrode.

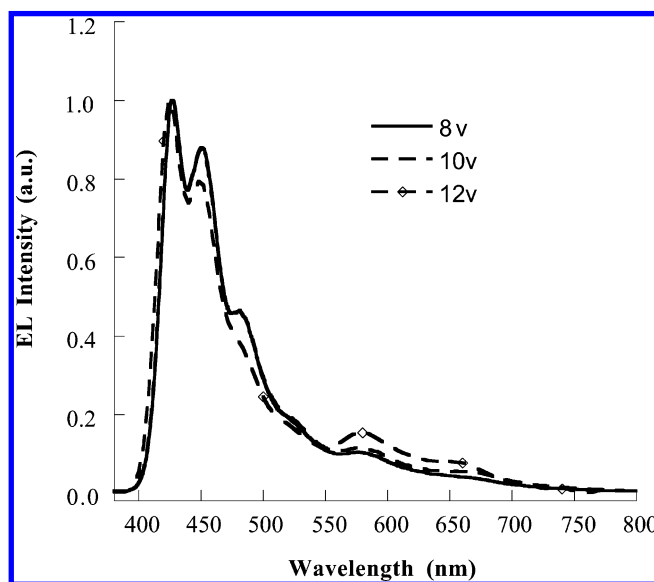


Figure 5. EL spectra measured for the ITO/PEDOT/PF-TPA-OXD/Ca/Ag device at different voltages.

the copolymer. These results from CV indicate that the incorporation of electron-rich TPA and electron-deficient OXD groups leads to an increase in both hole and electron affinities and an improvement in charge injection of the polymer.

Electrical Properties. The hole- and electron-transporting properties of this polymer were investigated using a “hole-only” or an “electron-only” configuration that contains a polymer layer sandwiched between ITO and Au and Al and Ca electrodes, respectively.²⁷ The J - E characteristics of these devices showed that PF-TPA-OXD possesses lower hole and electron conduction than those of POF. This may be due to that bulky substituents like TPA and OXD prevents polymer chain from packing together. As a result, it lowers the charge mobility.

Electroluminescence. A single-layer LED device with the configuration of ITO/PEDOT:PSS/PF-TPA-OXD/Ca/Ag was fabricated. The electroluminescence (EL) spectra show that the emission falls in the blue region with the CIE coordinates of (0.193, 0.141) (Figure 5). The new lower energy emission tail appeared in the

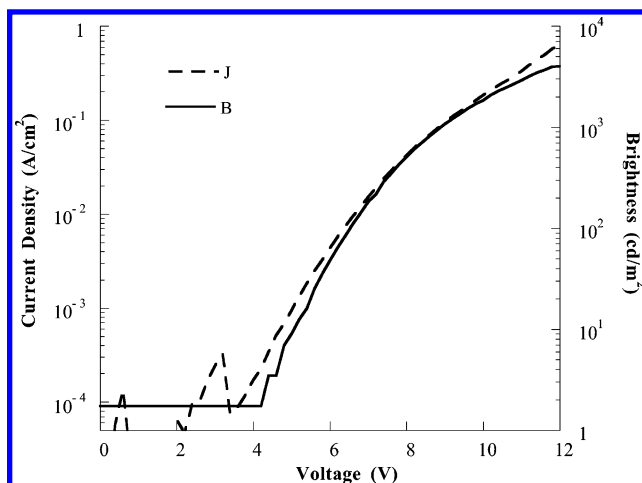


Figure 6. Current density–voltage–brightness (J - V - B) characteristics of the LED device.

EL spectra may be due to the formation of emissive fluorenone defects as a result of the electrooxidative degradation of dioctylfluorene units.²⁸ The rather low turn-on voltage of 4.4 V (defined as the voltage required to give a luminance of 1 cd/m^2) and low operation voltages suggest that TPA and OXD side chains function well for charge injection. The maximum external quantum efficiency of this device is 1.21% (at a brightness of 354 cd/m^2 with driving voltage of 7.6 V), which is more than 2 times higher than that of the previously reported device with PF-OXD as the emitting layer. The maximum luminance for bright blue emission as depicted in Figure 6 is found to be 4080 cd/m^2 (at a bias of 12.0 V and a current density of 640 mA/cm^2). The efficiencies at this luminance are 0.19 lm/W and 0.63 cd/A , respectively. The higher efficiency and brightness achieved in PF-TPA-OXD-based devices are due to better charge injection and more efficient charge recombination.

Conclusions

In conclusion, a highly efficient blue emitter, PF-TPA-OXD, with bipolar pendant groups at the C-9 position of fluorene was synthesized. The incorporation of electron-rich TPA and electron-deficient OXD groups leads to an increase in both hole and electron affinities. The polymer shows both a pure blue emission without the formation of aggregates/excimers and a balanced hole- and electron-injection/transport compared to those from the fluorene homopolymer (POF) and copolymer (PF-OXD), which has only the electron-deficient OXD as side chains.

Acknowledgment. C.-F. Shu thanks the National Science Council of the Republic of China for financial support. A. Jen thanks the Boeing-Johnson Foundation for financial support. M. Liu thanks support from the Joint Institute for Nanoscience funded by the Pacific Northwest National Laboratory (operated by Battelle for the U.S. Department of Energy) and the University of Washington.

References and Notes

- (1) Kido, J.; Hongawa, K.; Okuyama, K.; Nagai, K. *Appl. Phys. Lett.* **1994**, *64*, 815.
- (2) Kido, J.; Shionoya, H.; Nagai, K. *Appl. Phys. Lett.* **1995**, *67*, 2281.
- (3) McGehee, M. D.; Bergstedt, T.; Zhang, C.; Saab, A. P.; O'Regan, M. B.; Bazan, G. C.; Srdanov, V. I.; Heeger, A. J. *Adv. Mater.* **1999**, *11*, 1349.

- (4) Chen, F.-C.; Yang, Y.; Thompson, M. E.; Kido, J. *Appl. Phys. Lett.* **2002**, *80*, 2308.
- (5) Pei, Q.; Yang, Y. *J. Am. Chem. Soc.* **1996**, *118*, 7416.
- (6) Leclerc, M. *J. Polym. Sci., Part A: Polym. Chem.* **2001**, *39*, 2867.
- (7) Neher, D. *Macromol. Rapid Commun.* **2001**, *22*, 1365.
- (8) Becker, S.; Ego, C.; Grimsdale, A. C.; List, E. J. W.; Marsitzky, D.; Pogantsch, A.; Setayesh, S.; Leising, G.; Müllen, K. *Synth. Met.* **2002**, *125*, 73.
- (9) Grice, A. W.; Bradley, D. D. C.; Bernius, M. T.; Inbasekaran, M.; Wu, W. W.; Woo, E. P. *Appl. Phys. Lett.* **1998**, *73*, 629.
- (10) Kläner, G.; Davey, M. H.; Chen, W. D.; Scott, J. C.; Miller, R. D. *Adv. Mater.* **1998**, *10*, 993.
- (11) Setayesh, S.; Grimsdale, A. C.; Weil, T.; Enkelmann, V.; Müllen, K.; Meghdadi, F.; List, E. J. W.; Leising, G. *J. Am. Chem. Soc.* **2001**, *123*, 946.
- (12) Ego, C.; Grimsdale, A. C.; Uckert, F.; Yu, G.; Srdanov, G.; Müllen, K. *Adv. Mater.* **2002**, *14*, 809.
- (13) Pogantsch, A.; Wenzl, F. P.; List, E. J. W.; Leising, G.; Grimsdale, A. C.; Müllen, K. *Adv. Mater.* **2002**, *14*, 1061.
- (14) Marsitzky, D.; Vestberg, R.; Blainey, P.; Tang, B. T.; Hawker, C. J.; Carter, K. R. *J. Am. Chem. Soc.* **2001**, *123*, 6965.
- (15) Wu, F.-I.; Reddy, D. S.; Shu, C.-F.; Liu, M. S.; Jen, A. K.-Y. *Chem. Mater.* **2003**, *15*, 269.
- (16) Ranger, M.; Leclerc, M. *Macromolecules* **1999**, *32*, 3306.
- (17) Thayumanavan, S.; Barlow, S.; Marder, S. R. *Chem. Mater.* **1997**, *9*, 3231.
- (18) Ranger, M.; Rondeau, D.; Leclerc, M. *Macromolecules* **1997**, *30*, 7686.
- (19) Eaton, D. *Pure Appl. Chem.* **1998**, *60*, 1107.
- (20) Greenhan, N. C.; Friend, R. H.; Bradley, D. D. C. *Adv. Mater.* **1994**, *6*, 491.
- (21) Tokito, S.; Tanaka, H.; Noda, K.; Okada, A.; Taga, Y. *Appl. Phys. Lett.* **1997**, *70*, 1929.
- (22) Lee, J. I.; Klaerner, G.; Miller, R. D. *Synth. Met.* **1999**, *101*, 126.
- (23) Wu, F.-I.; Dodda, R.; Reddy, D. S.; Shu, C.-F. *J. Mater. Chem.* **2002**, *12*, 2893.
- (24) Förster, T. *Discuss. Faraday Soc.* **1959**, *27*, 7.
- (25) Pommerehne, J.; Vestweber, H.; Guss, W.; Mahrt, R. F.; Bäessler, H.; Porsch, M.; Daub, J. *Adv. Mater.* **1995**, *7*, 551.
- (26) Janietz, S.; Wedel, A. *Adv. Mater.* **1997**, *9*, 403.
- (27) Parker, I. D. *J. Appl. Phys.* **1994**, *75*, 1656.
- (28) Scherf, U.; List, E. J. W. *Adv. Mater.* **2002**, *14*, 477.

MA030123E